

# Hypothesis

## ***Brain Chip***

*Tsutomu Nakada*<sup>1</sup>

*Center for Integrated Human Brain Science  
Brain Research Institute, University of Niigata*

This article is the English version of the Brain Chip hypothesis previously presented in the books “Brain Equation One Plus One (Kinokuniya, 2001)” and “Plus Alpha (Kinokuniya, 2002).” The concept in this article has been translated into English by the author himself in response to an overwhelming number of requests from colleagues outside Japan.

Key Word: cerebellar chip, neural net, aquaporin-4, radial glial fiber, ELDER, CEO

### ***Introduction***

There is no doubt of the essential role of discrete neuronal networks in brain function. Nevertheless, models of brain function based on neuronal networks alone fail to answer the various fundamental questions of how the brain works, such as, “What is the neuronal substrate of consciousness?”, or “Why do anesthetic effects diminish at higher atmospheric pressure?”, or “How can purely endogenous processes be initiated?” These are but a few examples of as yet unsatisfactorily addressed questions. In spite of concerted effort by preeminent neuroscientists, no single complete theory of brain function explaining these phenomenologies has been offered. This void strongly suggests that there is a *missing link* in the current fundamental concept of how the brain works.

This apparent impasse in neuroscience has recently been surmounted by the Vortex Theory, which effectively links all important phenomenologies into a single fundamental concept of the brain’s functional organization (1). The theory is firmly based on biological and anatomical reality, essential considerations for any biological hypothesis. This manuscript is an introduction to the fundamental architectural unit of the association cortex in the Vortex

---

<sup>1</sup> Correspondence: Tsutomu Nakada, M.D., Ph.D., Center for Integrated Human Brain Science, Brain Research Institute, University of Niigata, 1 Asahimachi, Niigata 951-8585, JAPAN. Tel: (81)-25-227-0677, Fax: (81)-25-227-0821, e-mail: [tnakada@bri.niigata-u.ac.jp](mailto:tnakada@bri.niigata-u.ac.jp)

Theory, namely, the *brain chip*.

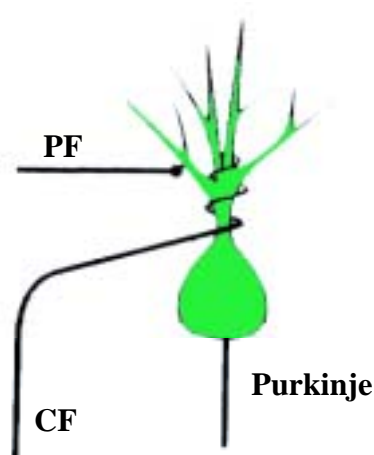
## *Developments*

### *Physiology*

Research on synaptic plasticity in the cerebellum has dramatically advanced the concept of brain function. The discovery of learning neurons confirmed the existence of the biological counterpart of Perceptron, an artificial neuron in the field of neural net and, in turn, provided virtual proof for the concept that, similar to artificial neural net, diverse functionality of the brain can be constructed based on a single functional unit. The concept of cerebellar learning was further refined by the identification of a physiologic biological functional unit, namely, the *cerebellar chip* (2).

A simplified representation of the cerebellar chip is given in Figure 1. The chip is organized around a single output neuron, the Purkinje cell. Information reaching the cerebellum is first processed by many, so termed, pre-processing neurons such as granular cells. The output of these pre-processing neurons reaches the Purkinje cells via the parallel fibers which form synaptic connections with dendrites of the Purkinje cells. Transmission efficacy of the synapses between parallel fibers and the Purkinje cells is modifiable, forming the basis of synaptic plasticity, and provides the biologic substrate of the cerebellar learning processes. The role of transmission efficacy in the learning process is analogous to the

**Figure 1: Cerebellar Chip**



Functionally, the cerebellum is now considered to be an organ collectively formed by identical functional units. The individual unit is referred to as “cerebellar chip”, in analogy to a computer chip. Each cerebellar chip has a single output neuron, the Purkinje cell. Information to the cerebellum is first processed by numerous preprocessing neurons, such as the granular cells, and eventually reaches the Purkinje cells via parallel fiber (PF) input. The transmission efficacy of the synapses between parallel fibers and Purkinje cells is modifiable, forming the basis of synaptic plasticity, and provides the substrate of the cerebellar learning process. The outcome of cerebellar system output is examined in other systems, and error signals are fed back to each Purkinje cell if the outcome is undesirable. These error signals are carried by the climbing fibers and provide the learning trigger for the corresponding Purkinje cells. Once a desirable outcome is achieved, the error signals will cease, and the learning process will be put on hold similar to the situation where the hold command is given to the McCulloch and Pitts neuron.

variable weights in the learning process of the McCulloch and Pitts neuron (Figure 2) (3).

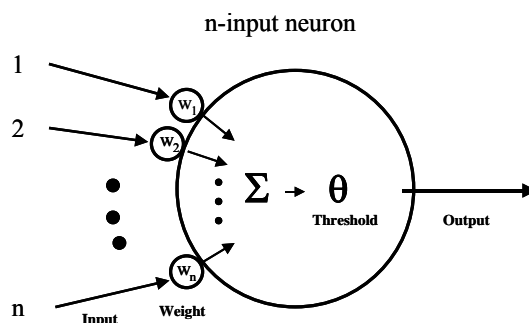


**Figure 2: McCulloch-Pitts classical linear model of the neuron**

At given time  $t$  input signals  $x_i(t)$  reach the synapses. Each input is transmitted through the synapse to the neuron after each has been modified by weight  $w_i$ . When the sum of the inputs reaches threshold  $\theta$ , the output of the neuron at time  $t+1$ ,  $y(t+1)$ , will become 1.

$$y(t+1) = \begin{cases} 1 & \text{if } \sum_i w_i x_i(t) \geq \theta \\ 0 & \text{if } \sum_i w_i x_i(t) < \theta \end{cases}$$

Patterns of ensemble firing of Purkinje cells represent the result of learning, and affects performance of a given behavior, such as eye movements. If a resultant behavior deviates from the original expectation, feedback signals will reach the corresponding *cerebellar chips* and effect changes in transmission efficacy, i.e. the learning process. The outcome of the cerebellar system output is examined in other systems, and error signals are fed back to each Purkinje cell if the outcome is undesirable. These error signals are carried by the climbing fibers and provide the learning trigger for the corresponding Purkinje cells. Once the desirable outcome is achieved, error signals will cease and the learning process will be put on hold, similar to the situation of the hold command given to the McCulloch and Pitts neuron.

Evolution is the result of inevitable events based on principles of nature. In this context, it is highly plausible that the basic organization of the cerebral cortex consists of single functional units as in the cerebellar cortex. Should such a unit, referred to here as *brain chip*, exist, it is likely to have evolved as an improved version of its predecessor, the *cerebellar chip*. It is therefore useful to examine carefully the basic anatomical architecture of the cerebral cortex in context of the *cerebellar chip*.

The cerebral cortex exhibits a basic neural architecture similar to the cerebellum. The

logical cerebral counterpart of cerebellar Purkinje cells are the pyramidal cells. There are numerous pre-processing neurons in the cerebral cortex which represent the counterpart of the granular cells in the cerebellum. Similar to the parallel fibers, axons of the small neurons in the cerebral cortex form synaptic connections with dendrites of the pyramidal cells, the transmission efficacy of which, even in the primary visual cortex, is highly plastic. One component missing in the cerebral cortex in the context of chip configuration is the equivalent structure to the cerebellar climbing fibers (Figure 3).

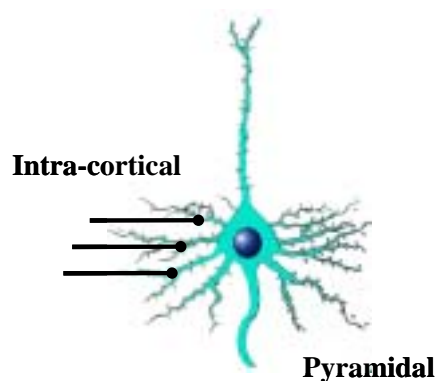


**Figure 3: Starting point of the Brain Chip**

Similar to the cerebellum, the cerebrum consists of numerous output neurons, the pyramidal cells. Their synapses, which receive various input signals from preprocessing neurons in the cortex through intracortical fibers, are highly plastic. A high degree of plasticity is observed even in the primary cortices, including the primary visual cortex. Should the functional unit of the cerebrum be organized similar to the cerebellar chip, such a functional unit, referred to here as “Brain Chip”, is expected to have a similar configuration. However, in comparison to the cerebellar chip, it is apparent that the cerebral cortex lacks climbing fibers. In this configuration, the learning trigger is missing in the cerebral cortex in this configuration.

### *Ontogeny*

Ontogenetic development of the cerebral cortex is phenomenologically well described. The cells which eventually form the six-layered cortex migrate from the surface of the lateral ventricle, the germinal matrix, following guiding tracts provided by the radial glial fibers (Figure 4). Each migrating cell reaches the surface of the cortex after first passing through all the previously migrated and settled cells, as if a six-story building were constructed beginning from the first story upward to the sixth (Figure 5). It is readily apparent that this

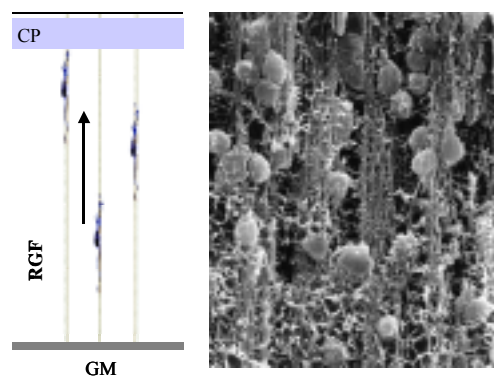


**Figure 4: Neuroblast delivery system**

Left: Schematic presentation of the process of neuroblast migration. RGF: radial glial fiber. GM: germinal matrix. CP: cortical plate. Right: Scanning electron-microscope picture depicting actual neuroblast migration. (Courtesy of Y. Ikuta (Professor Emeritus, University of Niigata).

process will not define the gross shape of the brain. Instead, the determining factor of the gross shape of the brain is the pattern of growth of the radial glial fibers (Figure 6) (4).

In nature, structural formation almost always follows the principal role of self-organization in Markovian fashion. Recently, I have provided virtual proof that the brain self-organizes based on the rule of free convection<sup>2</sup>. To follow the basic principles of

heat convection, radial glial fibers are only required to advance the tip of the fiber in the direction of convective heat flow (5). This process can be accomplished by the emission of small amounts of a gaseous substrate, such as nitric oxide (NO)<sup>3</sup> (Figure 7). The process can be seen as following a transparent blueprint drawn precisely to actual size. Each fiber tip advances to its destination by following the principal rule of heat convection governing the particular space in which the tip is located. Advancement of radial glial fibers, step-by-step, has been given previously.



**Figure 6: Schema for gross shape formation**

The gross shape of the brain is determined by how the glial fibers grow. In this schema, each fiber grows straight out from the center, forming a half-sphere.

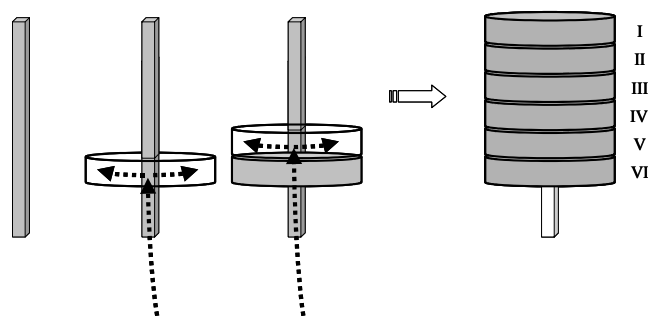


**Figure 5: Six-story building analogy**

The process of cerebral cortex formation is analogous to constructing a six-story building. First, a construction elevator is set up. The material for each floor is fabricated elsewhere, and is delivered to each floor by elevator. Upon completion of a floor, construction moves to the next level up. Once all six-stories are completed, the construction elevator is removed, leaving a space in the center of the building. In the brain, the radial glial fibers play the role of construction elevator. Following completion of brain formation, the radial glial fibers will disappear, leaving a space in the center of

<sup>2</sup> A brief description of this simulation study is given in the Appendix.

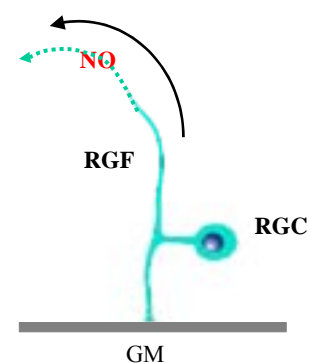
<sup>3</sup> NO has been implicated as one of the determining factor of brain development.

## Biology

Recent work has unambiguously shown that astrocytes are a cousin of neurons and derive from identical stem cells. The work provides impetus for the rigorous re-examination of astrocyte function. From the histological standpoint, there are two structures associated with astrocytes, the assembly and the electron dense layer. The role of these structures has long been enigmatic and poorly understood. Since nature seldom creates a structure without a corresponding specific function, it is prudent to analyze these structures for their potential role in brain function in regards to learning/information processing (Figure 8).

### Figure 7: Schema showing advancement of radial glial fibers

Schematic presentation of the proposed growth pattern of a radial glial fiber using nitric oxide (NO) as example. The tip of the growing radial glial fiber emits a gaseous substrate (NO in this figure), which flows based on the heat convection schema. The radial glial fiber grows in the direction of NO flow. GM: germinal matrix. RGF: radial glial fiber. RGC: radial glial cell.



The assembly is a protein structure found abundantly throughout the astrocyte cytoplasmic membrane. Recent studies indicate that this structure is identical to the water channel, aquaporin 4, found in great abundance in the collecting tubules of the kidney (6). These findings strongly indicate: (1) that one of the specific functions of astrocytes is related to the regulation of water contents in the brain; and (2) that the brain has compartments with differential water contents.

There is no doubt that the primary role of astrocytes is the physical support of neurons. The organizational characteristic of the astrocyte is matrix formation, which is an effective means of establishing compartments with different contents characteristics. This, together with the presence of water channels (aquaporin), make it highly plausible that astrocytes maintain two different types of extracellular compartments in the brain. The conventional extracellular space is filled with extracellular fluid, and indeed exists in certain structures where astrocytes effectively seal off an area in order to maintain a conventional extracellular fluid environment, e.g., the surroundings of the synaptic areas and the nodes of Ranvier. The second extracellular space, therefore, likely constitutes a dryer environment and lower water contents than conventional extracellular space (Figure 8).

Given that the astrocyte matrix is indeed composed of relatively dry components, the matrix can be conceptualized to represent biological Styrofoam. In other words, the astrocyte matrix has the perfect properties to function as molding material for protecting neuron networks.

The electron dense layer is a membrane-like structure formed by those astrocyte processes lining up immediately underneath the subpial basement membrane, at the surface of the brain. The unique presence of electrons, not negatively charged particles as in the case of the membrane potential, in unusually high-density, strongly indicates that this layer plays a role in electron flow, namely, current generation as will be elaborated below.

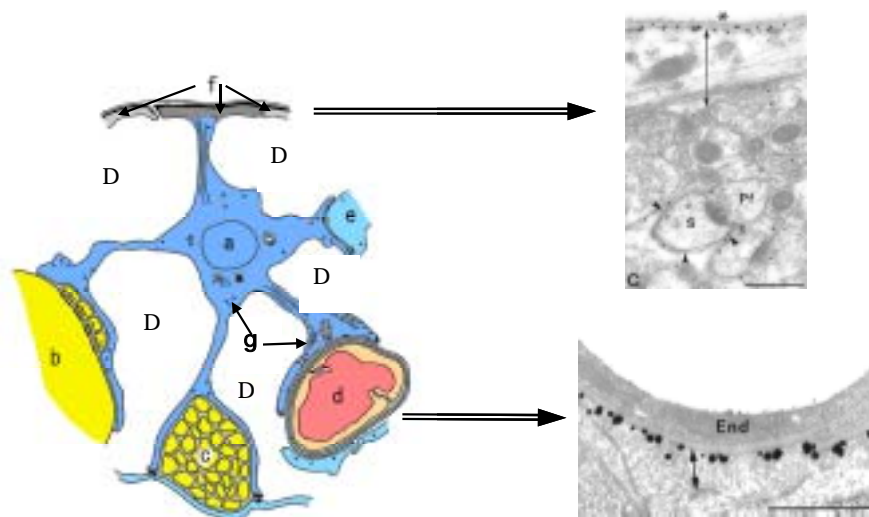


**Figure 8: Astrocytes and Aquaporin-4**

Left: Schematic presentation of an astrocyte and its principal processes. Modified and redrawn based on the figures from Hirano, 1999 and Sasaki, 1999. Astrocytes possess all the structural significance necessary for anatomical realization of the hypothesis. The key elements include: (1) electron rich layer formed by the principal processes just beneath the pia mater; (2) two compartments of extracellular spaces segregated by principal processes; and (3) assembly. “D” indicates “dry area”, the second extracellular space. See text for details. a: astrocyte, b: neuron, c: axon bundle, d: vessel, e: neighboring astrocyte, f: electron rich layer, g: assembly.

Right: Electron-microscopic picture depicting aquaporin-4 rich astrocyte processes. Upper: glia limitans; Lower: perivascular area. (Courtesy of J. Neeley. (Johns Hopkins University).

## *Proposals*

### *Synaptic Equivalence: ELDER*

The term “electron-dense” originally came from transmission electron-microscope observations that certain portions of membrane exhibited higher density. The finding implied that compared to other areas of the membrane, the electron dense membrane contained a much higher number of molecular elements that blocked the electron beam. Histologically, this layer (glia limitans) is formed by the footlike processes of the short fibers of fibrous astrocytes (marginal glia). Similar to perivascular regions, glia limitans is aquaporin rich. Therefore, it is highly plausible that glia limitans is effectively separated

from brain parenchyma by relatively dry space (Figure 8). Although the precise cellular characteristics of marginal glia and glia limitans are not understood, these observations point to one conclusion. Under the condition where intense dynamic electrical activities take place, for example, the cortex in live animals, the layer is likely to be charged because of the dielectric effect of the dry area. This implies that the “electron-dense layer”, originally coined as an electron microscopy term, is literally *electron dense* in life functioning brain and can play the role of electron donor.

The electron dense layer faces layer I of the cortex (molecular layer), which contains virtually all the terminal dendrites of the pyramidal cells regardless of their cell bodies location. The principal role of dendrites is to receive signals. The conventionally known means of signal transmission is synaptic transmission, which involves the conversion of chemical signals to electrical signals by dendrite receptors. As synthesis of the available information, I propose that there is a synapse-like structure at the surface of Layer I (molecular layer) termed ELDER<sup>4</sup>. While the electron dense layer plays the role of synaptic button, the dendritic ramifications represent the receptor. The space in between these two structures, ELDER gap, is a compartment the water contents of which is regulated by the assembly (Figure 9). Transmission in the ELDER system occurs as a function of permittivity changes of the ELDER gap based on transient water condensation to be discussed below.

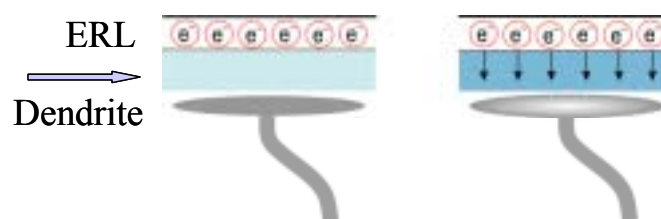


**Figure 9: ELDER**

Schematic presentation of the ELDER system. With the permittivity lower than threshold (left), there is no current (rest). The higher water density within the ELDER space increases permittivity. Once threshold is reached (right), current will be introduced (excitation). ERL: electron rich layer, just beneath of the pia matter, formed by astrocyte processes. Blue arrow: ELDER gap.

### *Synaptic Transmission Equivalent: Vortex-Entropy Waves*

As shown by the analogy to the six-story building (Figure 5), the cortex is built from the bottom up by adding layer on top of completed layer. The radial glial fibers play the role of “elevator” which transports necessary materials (neuroblasts) to the top of the completed floor. To optimize efficiency, it is highly conceivable that each building unit uses a single elevator located at the center of the building to be built. In brain development, a single radial glial

<sup>4</sup> *Electron-dense Layer and DEndritic Ramification.*

fiber is responsible for a single cortical column and is located at the center of the column.

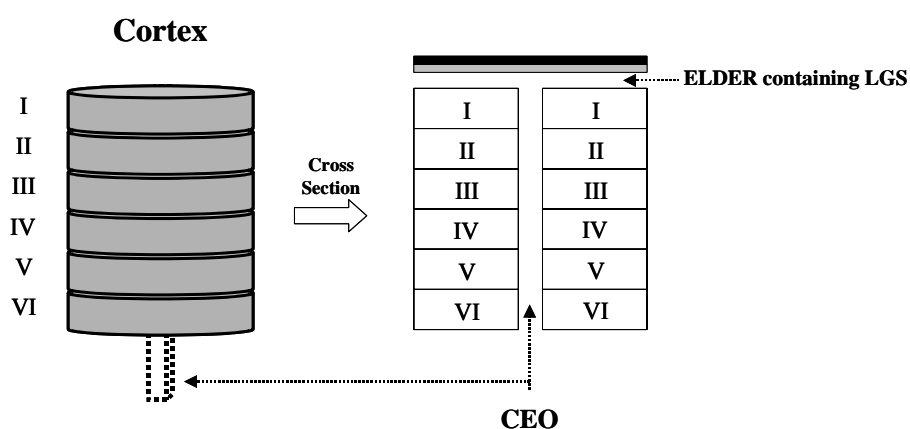


**Figure 10: Schema of CEO**

Radial glial fibers disappear following completion of cortical development, leaving a hollow, tract-like structure in the center of each cortical column (Figure 10). This tube-like space is conceived to be part of the second extracellular space, namely, dry space. This structure, which is referred to as CEO<sup>1</sup>, possesses the ideal configuration to serve as conduit for the dissipation of the tremendous amount of heat generated by the neuron networks, a biological air-cooling system. Note, the formation of CEO is based on the heat convection schema (see Appendix).

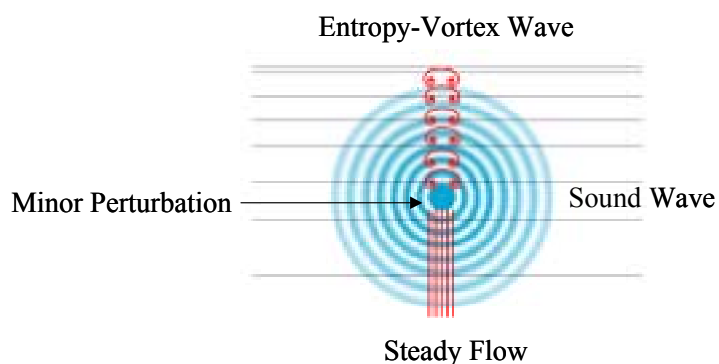


**Figure 11: Vortex and Sound waves**

Minor perturbation results in the formation of one entropy-vortex wave and one sound wave. The former travels in the direction identical to the original flow, whereas the latter radially in all directions. The entropy-vortex wave carries newly processed information ( $\delta s \neq 0$ ), while the sound wave does not ( $\delta s = 0$ ). See Appendix II.

Radial glial fibers disappear following completion of cortical development, leaving a hollow, tract-like structure in the center of each cortical column (Figure 10). This tube-like space is proposed be part of the second, dry extracellular space. This center structure, which is referred to as CEO<sup>5</sup>, has the ideal configuration to serve as conduit for dissipation of the tremendous amount of

<sup>5</sup> Climbing-fiber *Equivalence Organon*

heat generated by the neuron networks, a biological air-cooling system. It will be recalled that the formation of CEO is based on the heat convection schema (see Appendix).

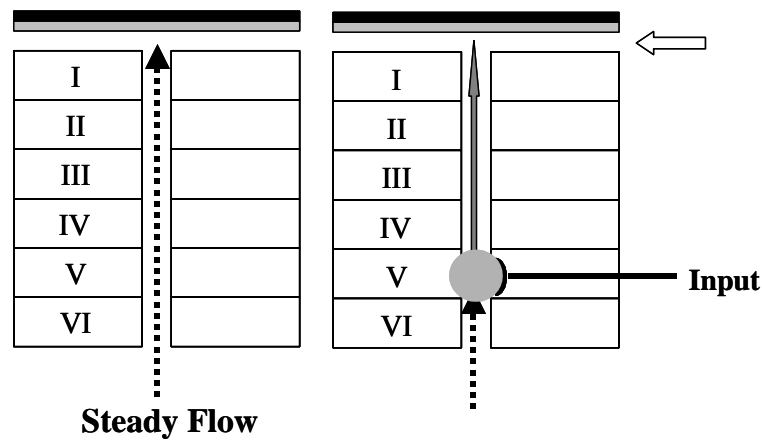


**Figure 12: Vortex Wave and CEO/LGS**

Schematic view of vortex wave formation by neural input within CEO. Minor perturbation of the steady flow due to arrival of a neural impulse results in vortex wave formation (right). The vortex wave travels in the direction identical to the original flow, namely, within the CEO, and towards LGS. See Figure 14 for schematic view of the area indicated by white arrow as seen from the ventral aspect of the brain.

Within CEO, there is a steady air flow driven by a steady state transfer of heat. When surfeit heat is generated by neuronal processing, an intriguing phenomenon will occur (Figure 11): the production of two waves, namely, an entropy-vortex wave and a sound wave (Appendix II). Since these waves are generated under subsonic conditions, the sound waves propagate radially in three dimensions. The entropy-vortex waves, however, move along the original flow, i.e., they travel within CEO towards the surface of the brain (Figure 12). Upon reaching the surface, these entropy-vortex waves meet the ELDER containing space at the center of the column, I term LGS<sup>6</sup> (Figure 13).

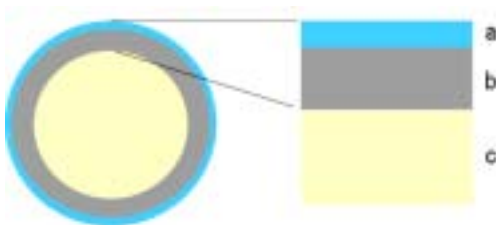


**Figure 13: Simplified view of the brain**

Schematic presentation of the dual processing shell system. a: lattice-gas shell, b: neural network shell, c: white matter and other deep structures.

At steady state, LGS has a steady flow. With the arrival of entropy-vortex waves, significant waves propagate outward from the center (Figure 14). The transient passage of

<sup>6</sup> *Lattice Gas Shell*

these waves increases the water contents of ELDER gaps sufficiently for electron transmission to occur, and results in the activation of a group pyramidal cells simultaneously. A certain type of Aquaporin channel may be activated by water (or CO<sub>2</sub>) density alteration and generate active release of water akin to conventional neurotransmitter release. In either case, water functions as neurotransmitter. Since waves decay as a function of distance, activation will be weighted based on the distance of pyramidal cells with respect to the center of the column (Figure 15). The process effectively provides a learning kernel equivalent to Kohonen's map (Appendix III).

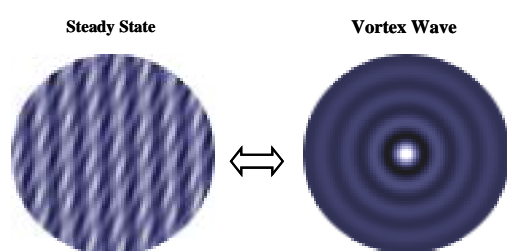


**Figure 14: Ripple vs. Vortex wave**

Under steady state, the dry space of LGS, which contains the ELDER space, shows non-organized ripples (left). With the arrival of a vortex wave to the center of a column, significantly organized waves will propagate outward from the center (right).

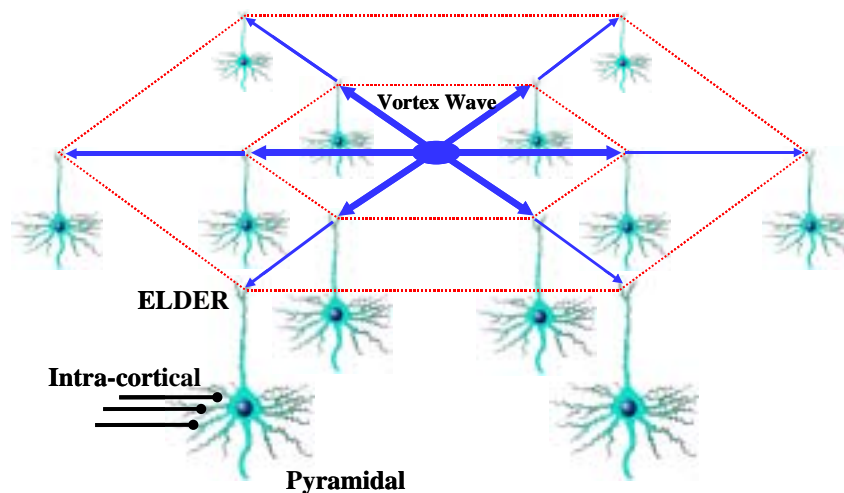


**Figure 15: Brain Chip**

The brain chip is a two-dimensional cerebellar chip where multiple pyramidal cells receive learning triggers simultaneously. In this schema two sets of six pyramidal cells are considered to form a single brain chip. Arrival of a vortex wave generates an organized wave propagating outward from the center, which activates multiple pyramidal cells simultaneously through ELDER activation. Since a wave decays as a function of distance, activation is weighted based on the distance of pyramidal cells from the center of the column.

## *Discussion*

### *Brain Chip: Biological Kohonen's Chip*

The human brain contains more than one hundred billion neurons and  $10^{14}$  synapses. Even without regard to the size of the genome, it can be easily concluded that a deterministic blueprint for connectivity of such an enormous number of networks is unrealistic. Therefore, as in the case of structure formation, self-organizing processes must play a significant role in developing functional connectivity of neurons. Among the many algorithms in neural net models, the concept generally referred to as Kohonen's self-organizing map, provides the most plausible self-organization processes for creating associative memories, the

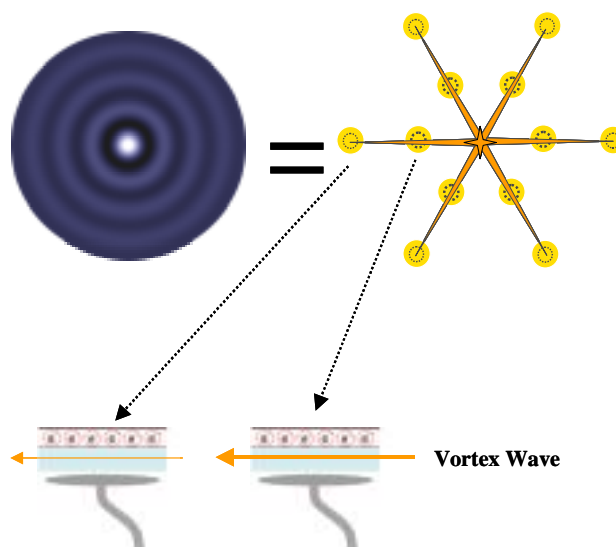


**Figure 16: Brain Chip as biological Kohonen's map**

Vortex waves in the brain chip play the equivalent role of climbing fibers in the cerebellar chip with one notable difference. The physics of a wave gives the brain chip a two dimensional property. At the same time, the vortex wave fulfills the condition necessary for the distance dependent learning weighting of Kohonen's map

configuration of which are virtually identical to that found in neurophysiological studies (7).

The CEO-LGS system fills the missing role of the climbing fibers equivalent in the cerebral cortex. The single column unit CEO, as schematically depicted in Figure 16, has the configuration of a two dimensional cerebellar chip. Instead of one to one activation of a Purkinje cell by a linearly connected climbing fiber as in the cerebellar chip, spatially graded activation through the ELDER system of a group of pyramidal cells within a single brain chip can be effectively achieved by the CEO-LGS system. This configuration is highly compatible with the self-organizing neural net of Kohonen type for effectively creating

associative memory, the configuration of which has been repeatedly validated by neurophysiological studies.

### *The Legacy of Linus C. Pauling*

Double Nobel Prize laureate (Chemistry and Peace), Linus Carl Pauling, was deeply intrigued by the fact that the inert gas, Xenon, was an excellent general anesthetic. He concluded that the only property common to all anesthetic agents, including Xenon, was their effect on water crystallization (8). The hydrate-microcrystal (aqueous-phase) theory did not receive significant attention. Nevertheless, as Pauling himself stated (9), “*the hydrate-microcrystal idea should be an important part of the accepted theory of general anesthesia when the theory is finally formulated.*” One of the main reasons why the hydrate-microcrystal theory did not receive nod of approval from scientific society was because Pauling incorrectly implied the effect of water condensation on neuronal membrane potentials. Had Pauling known the Vortex Model and brain chip theory, he would immediately have realized that water condensation within CEO and ELDER to be the critical factor.

Under the Vortex Theory/Brain Chip concept, the consciousness can be defined as the steady, random, spontaneous discharges of cortical pyramidal cells through ELDER mediated electron flow triggered by the steady flow of the CEO-LGS system. Establishment of a steady state within the LGS of the brain requires a certain thermodynamic steady state or homeostasis. The thermal gradients required to produce a convective force are dependent on the presence of an appropriately heated solid body core. In the context of the free convective self-organization schema, the reticular activation system (RAS), or reticular formation, and its connectivity within the thalamus likely play the primary role of a solid body with steady temperature for generating convective flow. The state of consciousness is dependent on the establishment of the requisite thermodynamics, and, resultant establishment of steady state cortical activities through the ELDER system.

A highly plausible explanation for the basic mechanism of anesthetic agents is, as Pauling anticipated, their effect on the kinetic viscosity (Reynold’s number) of a fluid or gas involved in propagating an essential steady flow because of water microcrystal formation. Such an alteration in kinetic viscosity produces alteration in the kinetics of the steady flow and, hence, ELDER activities. Pauling’s microcrystal theory also provides an answer to the long unsolved mystery in anesthesia: Why anesthetic effect is enhanced when the subject is placed in an environment of lower atmospheric pressure. Pauling had shown that hydrate microcrystal formation due to admixture with anesthetic agents, including alcohol, is dependent on atmospheric pressure. At lower atmospheric pressure, the identical concentration of an anesthetic agent results in more ready microcrystal formation.

### *Implication for functional MRI: Aquaporin as a mediator of autoregulation*

One of the regional phenomena known to occur in association with brain activities is the phenomenon generally referred to as autoregulation, the main feature of which is an increase in regional blood flow (11). Although the exact controlling mechanisms of autoregulation are not known, there have been many unambiguous observations of the coupling of physiological increase in regional blood flow and regional brain activities. In 1961 Sokoloff introduced autoradiographic images of the primary visual cortex exhibiting an increase in regional blood flow well corresponding to retinal stimulation (12). This observation became the world first “functional image”, and established the concept of brain activation study. The revolutionary advances in computer technology made possible for autoregulation based functional imaging, pioneered by Sokoloff, to be performed routinely in humans *non-invasively*. The first representative technology was positron emission tomography (PET), especially the one based on infusion of  $O^{15}$  labeled water ( $H_2O^{15}$ -PET).

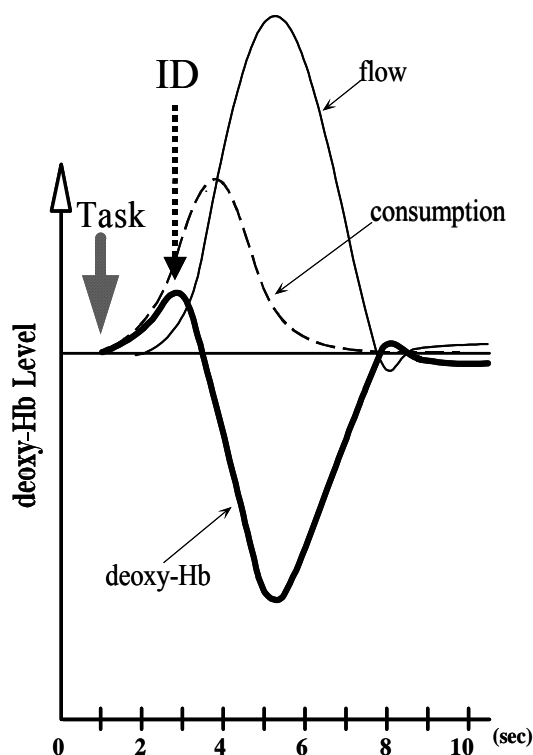


**Figure 17**

This simplified hypothesis states that oxygen supply in relation to an increase in activation-induced perfusion (flow in Figure) exceeds oxygen consumption associated with neuronal activities. As a result, regional deoxy-Hb levels paradoxically decrease in association with neuronal activities (brain activation). However, that regional deoxy-Hb decline associated with increase in regional blood flow can simply be explained by the well-known Munro-Kellie doctrine without additionally introducing the concept of oxygen consumption (see Figure 18). Accordingly, fMRI should be considered to be a blood flow based functional imaging method virtually identical to  $H_2O^{15}$ -PET.

Widely adopted fMRI methodologies detect pixels which show a statistically significant *increase* (not decrease) in signal intensity on T2\* weighted images. In other words, the technique detects a *decline* in relative deoxy-Hb concentrations in a given voxel. Since an increase in oxygen consumption associated with regional neural activities results in an *increase* in deoxy-Hb concentrations and, hence, a decline in signal intensity on T2 weighted images, fMRI in fact detects a phenomenon totally opposite to that predicted based on oxygen

consumption. The reverse observed phenomenon is generally attributed to an “oversupply of oxygen” brought about by an increase in regional blood flow (Figure 17) (13). Therefore,

$$A + V + \text{CSF} = \text{constant}$$

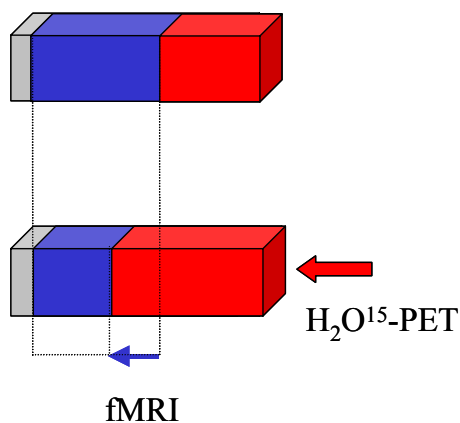


**Figure 18: Munro-Kellie doctrine**

the majority of, if not all, fMRI studies detect regional brain activities based on regional blood flow. It is well known that an increase in regional blood flow results in spontaneous reduction in venous blood volume in accordance with the Munro-Kellie doctrine (Figure 18) (14). It is clear that a decline in relative deoxy-Hb concentrations in a given voxel, the basis of fMRI, is readily explainable as a physiological epiphenomenon accompanying increase in regional blood flow, without the need to invoke changes in blood oxygenation. Like its sister methods, such as  $\text{H}_2\text{O}^{15}$ -PET, fMRI is another functional imaging method based on regional blood flow.

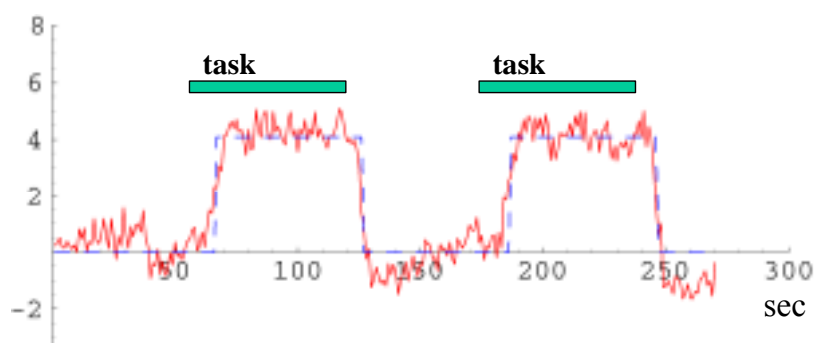


**Figure 19**

Typical time series of an activated pixel in the primary motor cortex. Red: raw data. Blue: boxcar type model function. Note the delay in activation signal changes compared to actual task performance.

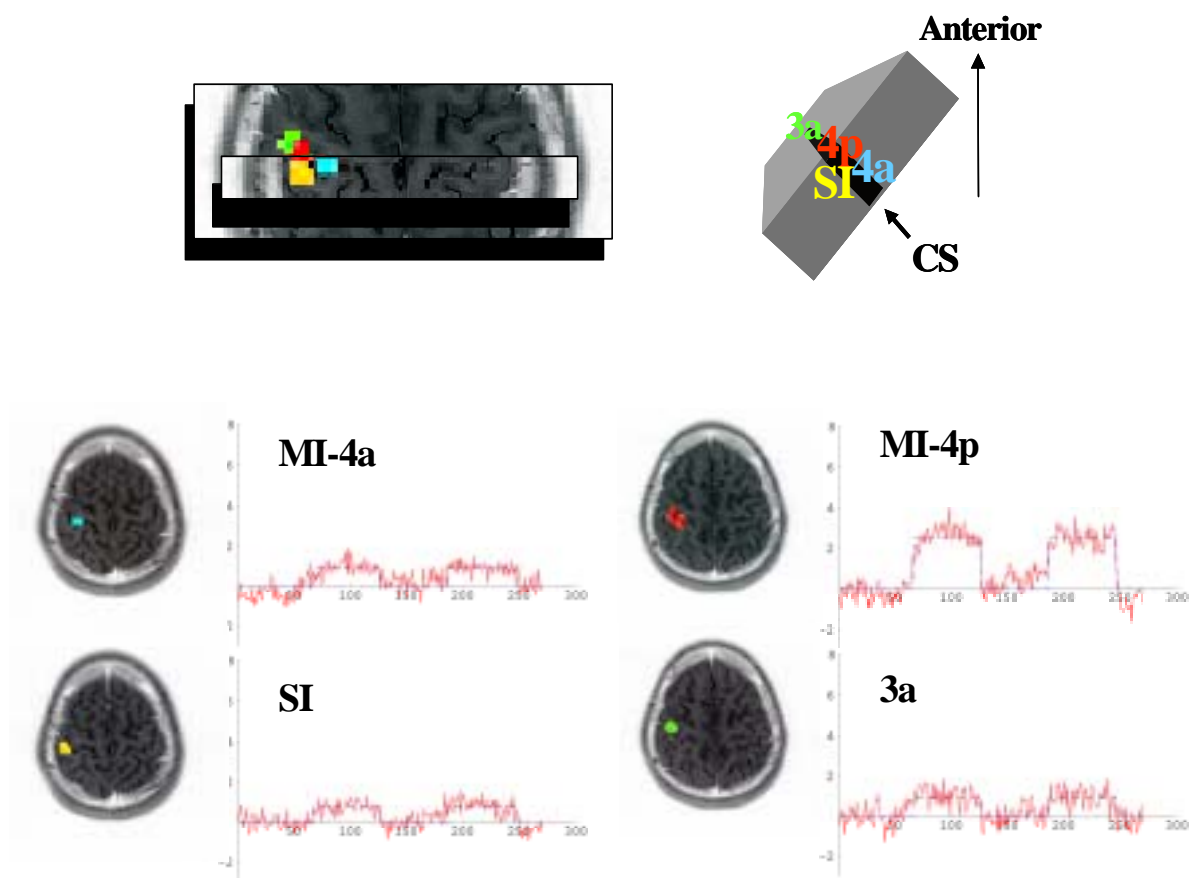


**Figure 20: Subdivision of primary motor cortex**

Representative independent component fMRI images within the right primary sensorimotor cortex (SMI) obtained by independent component-cross correlation-sequential epoch (ICS) analysis. The entire right SMI was covered by two consecutive 5 mm thick axial slices placed 2.5 mm apart. ICS analysis identifies functionally independent, spatially discrete components (independent component fMRI images). Activated areas are quantitatively color-coded according to the magnitude of activation using a differential color schema for each functionally discrete independent component. Red graphs indicate representative time series of independent components corresponding to the accompanying fMRI image. Blue lines represent the 6 second delayed boxcar model function applied to cross correlation analysis. The abscissa indicates time in seconds and the ordinate indicates percent mean intensity changes. MI-4a, 4 anterior area of the primary motor cortex; MI-4p, 4 posterior area of the primary motor cortex; 3a, 3a area of the primary sensory cortex; SI, the “classical” primary sensory cortex (Brodmann areas 1, 2 and 3b). To provide better visualization of the three dimensional (3D) relationship, part of the activation map of slice 1 is placed over that of slice 2 (upper left). The schematic gray block (upper right) shows the 3D spatial position of SMI and the localization of the independent areas of activation. CS: central sulcus. MI-4a, 4 anterior area of the primary motor cortex; MI-4p, 4 posterior area of the primary motor cortex; 3a, 3a area of the primary sensory cortex; SI, the “classical” primary sensory cortex (Brodmann areas 1, 2 and 3b).

What is the mechanism of neural activities associated increase in regional blood flow? Again, the vortex theory gives a highly plausible hypothesis of the molecular mechanisms of autoregulation, namely, temporal and spatial coupling of neural activity and blood flow. It is well known that the response in regional blood flow corresponding to neural activities shows a delay of four to six seconds (Figure 19). Nevertheless, once activated, increases in blood flow has a relatively low time constant consonant with flow changes associated with caliber changes in blood vessels. This indicates that the molecular mechanisms responsible for blood flow change possess at least two cascades of processes the final result of which is an increase in vessel caliber<sup>7</sup>. Vessels within the region of cortex which is the target of this discussion do not possess a muscular layer that controls vessel caliber. Therefore, theoretically, vessel caliber change can be accomplished by either: 1) increase in inflow controlled by the proximal arterial component resulting in increase vessel caliber due to passive changes in the flexible vessel walls; or 2) physical structure, as yet to be defined. One's intuition may accept the former. Several studies, however, indicate that regional flow changes coupled with given neural activities occur in the order of less than 1 mm<sup>3</sup> (Figure 20), clearly indicating that the former possibility is *not* the case. Accordingly, one has to accept the latter, requiring identification of non-muscular structures responsible for caliber changes. The best candidate is aquaporin-4 (assembly) regulated water contents of the structures surrounding vessels. Such a structure is astrocyte feet (Figure 8).

According to the Vortex Theory (1), one of the main constituents of the fluid flowing within the COE and LGS is likely to be CO<sub>2</sub><sup>8</sup> (REF). Following arrival of input, an entropy-vortex wave is created and travels along the CEO (Figure 12). If CO<sub>2</sub> content within the fluid is at near saturation, this perturbation results in release of CO<sub>2</sub> from the fluid analogous to champagne stirred by a bubble cutter (Figure 21). How aquaporin-4 (assembly) will be activated is not totally understood at this point. Nevertheless, accumulating data suggest two potential candidates, namely, water molecules and



**Figure 21: Champagne and bubble cutter**

Women often carried a bubble cutter for drinking champagne at social functions in order to be spared the embarrassment of eructating, or burping, in public.

<sup>7</sup> Readers are reminded that this discussion is for regional blood flow, not for regional blood volume.

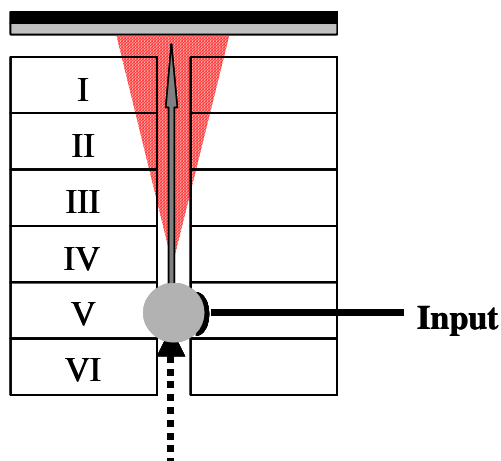
<sup>8</sup> There are several reasons to believe that CO<sub>2</sub> would be the primary gas within the dry area. High concentrations of carbonic anhydrase in oligodendroglia may indeed reflect this functionality.

CO<sub>2</sub>.

Carbon dioxide (CO<sub>2</sub>), rather than oxygen (O<sub>2</sub>), is believed to have an important role in regional blood flow alteration (11,15). Should aquaporin-4 surrounding vessels indeed be regulated by CO<sub>2</sub>, the physical pressure imposed on vessels by astrocyte feet could be reduced resulting in increased blood flow (Figure 22). This can effectively explain the observed spatial and temporal coupling of neural activities and blood flow (autoregulation).

**Figure 22**

Similar to the release of bubbles into the air effected by stirring champagne using a bubble cutter, an entropy-vortex wave (solid arrow) can release CO<sub>2</sub> (red) from extracellular fluid where CO<sub>2</sub> is under near saturation. While the entropy-vortex wave introduces activation of ELDER, CO<sub>2</sub> can also affect aquaporin channels of surrounding vessels, thereby effectively producing coupling of neural activities and blood flow with spatial as well as temporal concordance.



### *Acknowledgement*

The work is supported by grants from the Ministry of Education, Culture, Sports, Science, and Technology (Japan). The manuscript is presented in part at the Center of Excellence (COE) Hearing, National Council of Science (Japan), June 2000 and the 32nd Annual Meeting of the Society for Neuroscience, Orlando, FL, 2002.

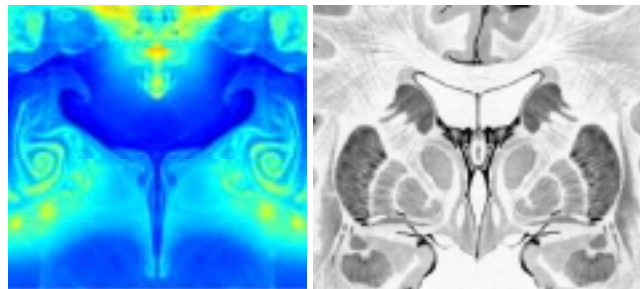
## *Appendix I*

### **Heat Convection Schema and Brain Shape**

Three-dimensional simulation of free convection was performed using an SGI Origin-2000, 64 CPU system. The governing equations in Eulerian form are given as:

$$\begin{aligned}\frac{\partial}{\partial t}\rho + \nabla \cdot (\rho \mathbf{v}) &= 0 \\ \frac{\partial}{\partial t}(\rho \mathbf{v}) + \nabla \cdot (\rho \mathbf{v})\mathbf{v} + \nabla p &= \mathbf{F} \\ \frac{\partial}{\partial t}(\rho \varepsilon) + \nabla \cdot (\rho \varepsilon \mathbf{v}) + \nabla(p\mathbf{v}) &= G + \rho \mathbf{v} \cdot \mathbf{F} \\ \text{where } \varepsilon &= \frac{\mathbf{v} \cdot \mathbf{v}}{2} + \frac{(\gamma - 1)^{-1} p}{\rho}\end{aligned}$$

where  $\varepsilon$  is the total specific energy,  $\rho$ , mass density,  $p$ , pressure,  $\mathbf{F}$  and  $G$ , momentum source and energy source, respectively, and,  $\gamma$ , the ratio of specific heats. Representative examples of two-dimensional “slice” images of consecutive steps of the simulation are sampled and shown in Figure 17. Details of the process are reported previously (5).



Simulation

Schematic

**Figure 23: Heat convection and brain shape**

A representative example of simulation results based on free convection. Due to imperfection of the selected initial conditions, the simulated image (simulation) is not wholly identical to an actual brain (Schematic). Nevertheless, the striking similarities in structural detail are demonstrated, strongly indicating that brain organization indeed follows the self-organization schema of free convection.

## *Appendix II*

### **Entropy-Vortex Wave**

Euler's equation is given by:

$$\frac{\partial \delta \mathbf{v}}{\partial t} + (\mathbf{v} \cdot \nabla) \delta \mathbf{v} + \frac{1}{\rho} \nabla \delta p = 0$$

where  $\delta \mathbf{v}$  and  $\delta p$  represent small perturbations in velocity and pressure, respectively.

Similarly, conservation of entropy and the equation of continuity give:

$$\frac{\partial \delta s}{\partial t} + \mathbf{v} \cdot \nabla \delta s = 0$$

$$\frac{\partial \delta p}{\partial t} + \mathbf{v} \cdot \nabla \delta p + \rho c^2 \nabla \cdot \delta \mathbf{v} = 0$$

where  $\delta \rho = \frac{\delta p}{c^2} + \left(\frac{\partial \rho}{\partial s}\right)_p \delta s$  and  $c$  represent sound velocity.

For a perturbation having the form  $\exp[i\mathbf{k} \cdot \mathbf{r} - i\omega t]$ , one gets:

$$(\mathbf{v} \cdot \mathbf{k} - \omega) \delta s = 0$$

$$(\mathbf{v} \cdot \mathbf{k} - \omega) \delta \mathbf{v} + \mathbf{k} \frac{\delta p}{\rho} = 0$$

$$(\mathbf{v} \cdot \mathbf{k} - \omega) \delta p + \rho c^2 \mathbf{k} \cdot \delta \mathbf{v} = 0$$

This result prescribes that there will be two types of perturbations, namely, entropy-vortex wave and sound wave, as defined below.

#### *Entropy-Vortex Wave*

$$\omega = \mathbf{v} \cdot \mathbf{k}$$

$$\delta s \neq 0$$

$$\delta p = 0$$

$$\delta \rho = \left(\frac{\partial \rho}{\partial s}\right)_p \delta s$$

$$\mathbf{k} \cdot \delta \mathbf{v} = 0$$

$$\nabla \times \delta \mathbf{v} = i\mathbf{k} \times \delta \mathbf{v} \neq 0$$

*Sound Wave*

$$(\omega - \mathbf{v} \cdot \mathbf{k})^2 = c^2 k^2$$

$$\delta s = 0$$

$$\delta p = c^2 \delta \rho$$

$$(\omega - \mathbf{v} \cdot \mathbf{k}) \delta p = \rho c^2 \mathbf{k} \cdot \delta \mathbf{v}$$

$$\mathbf{k} \times \delta \mathbf{v} = 0$$

For the purpose of brain modeling, the following points are emphasized: (1) for entropy-vortex wave,  $\delta s \neq 0$  and  $\omega = \mathbf{v} \cdot \mathbf{k}$ ; and (2) for sound wave,  $\delta s = 0$ . These conditions predict that a perturbation can produce entropy changes ( $\delta s \neq 0$ ) and, hence, information processing, and create entropy-vortex waves. The fact,  $\omega = \mathbf{v} \cdot \mathbf{k}$ , ensures that an entropy-vortex wave, which carries newly processed information, travels only in the direction identical to the original flow (10).

### Appendix III

#### Kohonen's Self-organizing Map

One of the most successful neural net applications for the creation of associative memories similar to that observed in brain, *in vivo*, is the self-organizing map (SOM) initially introduced by Kohonen, a non-linear method based on unsupervised learning processes.

A schematic presentation of the SOM is shown in Figure 18. Any point on the two dimensionally spread neural lattice can be excited.

For each input  $\mathbf{x}$ , the learning processes are confined to a local group of neurons centered at site  $s$ , where maximum adaptation occurs. The adaptive changes will decay according to their distance from the center (Neighborhood kernel) in Gaussian fashion.

$$h_{rs} = \exp\left(-\frac{\|r - s\|^2}{\sigma^2}\right)$$

Assuming active, non-linear forgetting,  $\varepsilon$ , occurs, the learning rule of each synapse can be given as:

$$\mathbf{w}_r^{(new)} = (1 - \varepsilon \cdot h_{rs}) \mathbf{w}_r^{(old)} + \varepsilon \cdot h_{rs} \cdot \mathbf{x} .$$

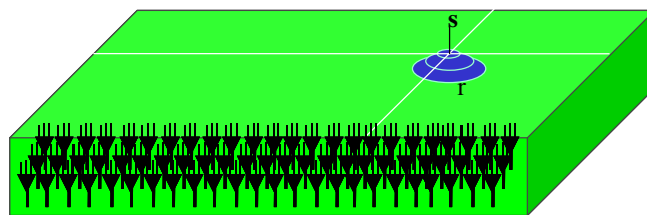


Figure 24

## *References*

1. Nakada, T. Vortex model of the brain: the missing link in brain science? In: T. Nakada (Ed.), *Integrated Human Brain Science*. Amsterdam: Elsevier, 2000: 3-22.
2. Ito M. Long-term depression: Characterization, signal transduction, and functional roles. *Physiol Rev* 2001;81:1143-1195.
3. Arbib MA (ed.): *The Handbook of Brain Theory and Neural Networks*. Massachusetts: The MIT Press, 1995.
4. Rakic P. Radial glial cells: scaffolding for brain construction. In H. Kettenmann and B. R. Ransom (Eds.) *Neuroglia* New York: Oxford University Press, 1995: 746-762.
5. Nakada T. Free convection schema defines the shape of the human brain: brain and self-organization. *Med Hypo* 2003;60:159-164.
6. Rash JE, Yamamura T, Hudson CS, Agre P, Nielsen S. Direct immunogold labeling of aquaporin-4 in square arrays of astrocyte and ependymocyte plasma membranes in rat brain and spinal cord. *Proceed Natl Acad Sci* 1998;95:11981-11986.
7. Kohonen T: *Self-Organizing Maps*. Third Edition. Berlin, Heidelberg, Springer, 2001.
8. Pauling L. A molecular theory of general anesthesia. *Science* 1961;134:15-21.
9. Marinacci B (ed.): *Linus Pauling in his own words*. New York, Touchstone, 1995.
10. Landau LD, Lifshitz EM: *Fluid Mechanics Second Edition*. Oxford, Pergamon Press, 1987.
11. Edvinsson L, Krause D. N. *Cerebral Blood Flow and Metabolism* Second Edition. Philadelphia, Lippincott Williams & Wilkins, 2002.
12. Sokoloff L. Local cerebral circulation at rest and during altered cerebral activity induced by anesthesia or visual stimulation. In Kety S. S., Elkes J. (Eds.): *The Regional Chemistry, Physiology and Pharmacology of the Nervous System*. Oxford, Pergamon Press, 1961:107-117.
13. Malonek D, Grinvald A. Interactions between electrical activity and cortical microcirculation revealed by imaging spectroscopy: Implication for functional brain mapping. *Science* 1996;272:551-554.
14. Sokoloff L. A historical review of developments in the field of cerebral blood flow and metabolism. In Fukuuchi (??) Y., Tomita M., and Koto A. (Eds.): *Keio University International Symposium for Life Sciences and Medicine, Volume 6, Ischemic Blood Flow in the Brain*. Tokyo, Springer-Verlag, 2001:3-10
15. Reivich M. Arterial Pco<sub>2</sub> and cerebral hemodynamics. *Am J Physiol* 1964;206:25-35.